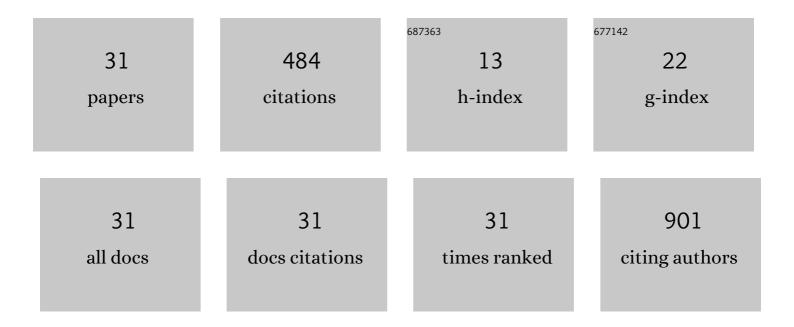
J HernÃ;ndez-Saz

List of Publications by Year in descending order

Source: https://exaly.com/author-pdf/5568884/publications.pdf Version: 2024-02-01



#	Article	lF	CITATIONS
1	Size effect and scaling power-law for superelasticity in shape-memory alloys at the nanoscale. Nature Nanotechnology, 2017, 12, 790-796.	31.5	70
2	Novel Method of Preparation of Goldâ€Nanoparticleâ€Doped TiO ₂ and SiO ₂ Plasmonic Thin Films: Optical Characterization and Comparison with Maxwell–Garnett Modeling. Advanced Functional Materials, 2011, 21, 3502-3507.	14.9	55
3	Small-pore driven high capacitance in a hierarchical carbon via carbonization of Ni-MOF-74 at low temperatures. Chemical Communications, 2016, 52, 9141-9144.	4.1	51
4	Heterometallic Titanium–Organic Frameworks by Metal-Induced Dynamic Topological Transformations. Journal of the American Chemical Society, 2020, 142, 6638-6648.	13.7	40
5	Synthesis of all equiatomic five-transition metals High Entropy Carbides of the IVB (Ti, Zr, Hf) and VB (V, Nb, Ta) groups by a low temperature route. Ceramics International, 2020, 46, 21421-21430.	4.8	34
6	Development of Surface-Coated Polylactic Acid/Polyhydroxyalkanoate (PLA/PHA) Nanocomposites. Polymers, 2019, 11, 400.	4.5	29
7	Insights into Preformed Human Serum Albumin Corona on Iron Oxide Nanoparticles: Structure, Effect of Particle Size, Impact on MRI Efficiency, and Metabolization. ACS Applied Bio Materials, 2019, 2, 3084-3094.	4.6	27
8	CVD synthesis of carbon spheres using NiFe-LDHs as catalytic precursors: structural, electrochemical and magnetoresistive properties. Journal of Materials Chemistry C, 2016, 4, 440-448.	5.5	22
9	Purcell Enhancement and Wavelength Shift of Emitted Light by CsPbI ₃ Perovskite Nanocrystals Coupled to Hyperbolic Metamaterials. ACS Photonics, 2020, 7, 3152-3160.	6.6	22
10	Microstructure, electrical and mechanical properties of Ti2AlN MAX phase reinforced copper matrix composites processed by hot pressing. Materials Characterization, 2021, 171, 110812.	4.4	21
11	Light Emission from Nanocrystalline Si Inverse Opals and Controlled Passivation by Atomic Layer Deposited Al ₂ O ₃ . Advanced Materials, 2011, 23, 5219-5223.	21.0	17
12	A methodology for the fabrication by FIB of needle-shape specimens around sub-surface features at the nanometre scale. Micron, 2012, 43, 643-650.	2.2	15
13	Atom-scale compositional distribution in InAlAsSb-based triple junction solar cells by atom probe tomography. Nanotechnology, 2016, 27, 305402.	2.6	13
14	3D compositional analysis at atomic scale of InAlGaAs capped InAs/GaAs QDs. Scripta Materialia, 2015, 103, 73-76.	5.2	12
15	Strain balanced quantum posts. Applied Physics Letters, 2011, 98, 173106.	3.3	7
16	Defect reduction in heteroepitaxial InP on Si by epitaxial lateral overgrowth. Materials Express, 2014, 4, 41-53.	0.5	7
17	Atom probe tomography analysis of InAlGaAs capped InAs/GaAs stacked quantum dots with variable barrier layer thickness. Acta Materialia, 2016, 103, 651-657.	7.9	6
18	Influence of the additivation of graphene-like materials on the properties of polyamide for Powder Bed Fusion. Progress in Additive Manufacturing, 2018, 3, 233-244.	4.8	6

J HernÃindez-Saz

#	Article	IF	CITATIONS
19	Pore morphology evolution and atom distribution of doped Fe2O3 foams developed by freeze-casting after redox cycling. Journal of Materials Research and Technology, 2021, 13, 1887-1898.	5.8	6
20	Influence of the growth temperature on the composition distribution at sub-nm scale of InAlAsSb for solar cells. Journal of Alloys and Compounds, 2018, 763, 1005-1011.	5.5	4
21	Analysis of the 3D distribution of stacked self-assembled quantum dots by electron tomography. Nanoscale Research Letters, 2012, 7, 681.	5.7	3
22	Strain analysis for the prediction of the preferential nucleation sites of stacked quantum dots by combination of FEM and APT. Nanoscale Research Letters, 2013, 8, 513.	5.7	3
23	Mapping the plasmonic response of gold nanoparticles embedded in TiO ₂ thin films. Nanotechnology, 2015, 26, 405702.	2.6	3
24	Gaussian kernel density functions for compositional quantification in atom probe tomography. Materials Characterization, 2018, 139, 63-69.	4.4	3
25	Strain balanced quantum posts for intermediate band solar cells. , 2010, , .		2
26	Effect of the thermal annealing and the nominal composition in the elemental distribution of InxAl1-xAsySb1-y for triple junction solar cells. Journal of Alloys and Compounds, 2019, 792, 1021-1027.	5.5	2
27	Simulation of transmission electron microscopy images using a generalized single-slice approach: The case of self-assembled quantum dots. Materials Characterization, 2020, 164, 110312.	4.4	2
28	Alumina doped Fe2O3 foams by freeze-casting for redox cycling applications. Journal of the European Ceramic Society, 2022, 42, 5922-5931.	5.7	2
29	Compositional Mapping by Z-Contrast Imaging. Microscopy and Microanalysis, 2011, 17, 1728-1729.	0.4	0
30	Fabrication of Needle-Shaped Specimens Containing Subsurface Nanostructures for Electron Tomography. Lecture Notes in Nanoscale Science and Technology, 2013, , 241-266.	0.8	0
31	THE USE OF AUDIO-VISUAL MATERIAL PRODUCED BY STUDENTS AS A TOOL IN THE LEARNING PROCESS. , 2018, , .		0